Biochimica et Biophysica Acta 1847 (2015) 126–133

Contents lists available at ScienceDirect

Biochimica et Biophysica Acta

journal homepage: www.elsevier.com/locate/bbabio

Review

Infrared spectroscopic markers of quinones in proteins from the respiratory chain☆

Petra Hellwig

Laboratoire de bioélectrochimie et spectroscopie, UMR 7140, Chimie de la matière complexe, Université de Strasbourg, 1, rue Blaise Pascal, 67008 Strasbourg, France

ARTICLE INFO

Article history:
Received 9 May 2014
Received in revised form 3 July 2014
Accepted 7 July 2014
Available online 12 July 2014

Keywords:
Quinone
FTIR spectroscopy
Electrochemistry
bd oxidase
Quinol oxidase
bc_1 complex

ABSTRACT

In bioenergetic systems quinones play a central part in the coupling of electron and proton transfer. The specific function of each quinone binding site is based on the protein–quinone interaction that can be described by means of reaction induced FTIR difference spectroscopy, induced for example by light or electrochemically. The identification of sites in enzymes from the respiratory chain is presented together with the analysis of the accommodation of different types of quinones to the same enzyme and the possibility to monitor the interaction with inhibitors. Reaction induced FTIR difference spectroscopy is shown to give an essential information on the general geometry of quinone binding sites, the conformation of the ring and of the substituents as well as essential structural information on the identity of the amino-acid residues lining this site. This article is part of a Special Issue entitled: Vibrational spectroscopies and bioenergetic systems.

1. Introduction

The quinone/quinol (Q/QH_2) couple is a key player in bioenergetic processes such as respiration and photosynthesis [1]. Quinones function as electron carriers between membrane proteins, thereby coupling electron transfer to the formation of a transmembrane proton gradient or acting as simple electron transfer partners. The different redox functions found for example for QA and QB in bacterial reaction centers or the bc_1 complex, as well as the accommodation of different quinone types observed in some bacteria, depending on growing conditions, are testimony to the flexibility of quinones in biological processes that is modulated by quinone–protein interactions. The investigation of protein–quinone interactions on molecular level is thus crucial for the understanding of the underlying reaction mechanisms.

Infrared spectroscopy is a sensitive method that is extensively used to study the structural changes that accompany the redox reaction of the quinones. The vibrational modes of the quinones in their different redox and protonation states serve as reporter groups for steric and energetic factors such as hydrogen bonding, polar interactions, and the distortion of ring and substituents. Hydrogen bonding interactions can be expected between the carbonyls of the quinone and proton-donating groups from amino acids. The specific perturbation of these interactions in site directed mutants is used for the analysis of the binding site of the quinone or an inhibitor. One of the main limitations of this technique, however, is that vibrational modes from all the bonds from both, the cofactor and the protein are due to contribute, leading to dense spectra with overlapping contributions.

Most studies performed on quinones in the respiratory chain have thus been performed by using reaction induced FTIR difference spectroscopy. The first reaction induced FTIR difference spectroscopic studies were presented by researchers working on bacteriorhodopsin and on photosynthesis [2–7]. Other applications then followed. Several approaches have been exploited to obtain difference FTIR spectra of quinones within proteins or in solution driving the redox reaction by light or electrochemically (for reviews see [8–11]). The difference spectra obtained represent the total of the molecular changes concomitant with the induced reaction, including conformational changes or charge redistributions at the cofactor sites. Importantly, proton reactions concomitant with electron transfer can be expected to contribute in the spectra.

The success of this approach is based on the possibility of monitoring the vibrational absorption band of a single functional group in a protein which contains the order of 100 or even more residues. The data reported is typically obtained by cycling the reaction of interest and averaging a large number of scans and cycles. The analysis is then based on the presence of specific vibrational marker modes of reactant, intermediate or product states. Isotopic substitution is often used to reveal the involvement of certain groups in the studied

Abbreviations: UQ, ubiquinone; MQ, menaquinone; FTIR, Fourier transform infrared spectroscopy; Q, quinone; QH_2, quinol; QFR, quinol fumarate reductase

☆ This article is part of a Special Issue entitled: Vibrational spectroscopies and bioenergetic systems.

E-mail address: hellwig@unistra.fr.

http://dx.doi.org/10.1016/j.bbabio.2014.07.004
0005-2728/

vibrational motions. Additional techniques for the analysis of the data are predictions from quantum chemical calculations or simulations. Current quantum chemical calculation routines, such as density functional theory (DFT), allow for the estimation of the electronic ground state structure of medium-sized molecules and have been extensively used together with simulation techniques for the analysis of quinone spectra [12–16].

One possibility for developing an understanding of the vibrational marker bands in the infrared is to first consider spectra of the relevant quinones in solution. In the following paragraphs the vibrational signature of the Q/QH_2 couple will be described and then corroborated with studies on quinone–protein interaction in proteins from respiration.

2. Infrared spectroscopic signatures of isolated quinones

2.1. Infrared spectra on oxidized quinones

The first published attempt at a complete vibrational assignment of quinones was made by Anno and Sado [17] who obtained infrared spectra of quinone solutions. Since then a significant number of studies on the vibrational properties of quinones were made describing the signal characteristic for the different redox states, the influence of isotope labeling, and comparing the different types of quinones. Several studies include the calculation of the quinone spectral properties. Here we will focus on ubi- and menaquinone, since they are the most commonly found in respiration.

Fig. 1 shows the absorption spectra of UQ_{10} and MQ (vitamin K^1). The most prominent signal of UQ seen between 1660 and 1640 cm^{-1} includes the coordinates of the ν(C═O) vibration [13,17–21]. The broadness of the signal of the isolated Q in solution points towards the presence of several interaction partners of C═O group with water. Upon binding to the protein, the signal often gets sharper. The exact position of the signal depends on the hydrogen bonding environment and on the geometry of the quinone binding site and is thus an important probe for the site. Table 1 summarizes the frequencies identified in different proteins from the respiratory chain and compares it to data reported for QA and QB sites in bacterial reaction centers and other proteins from photosynthesis studies. The

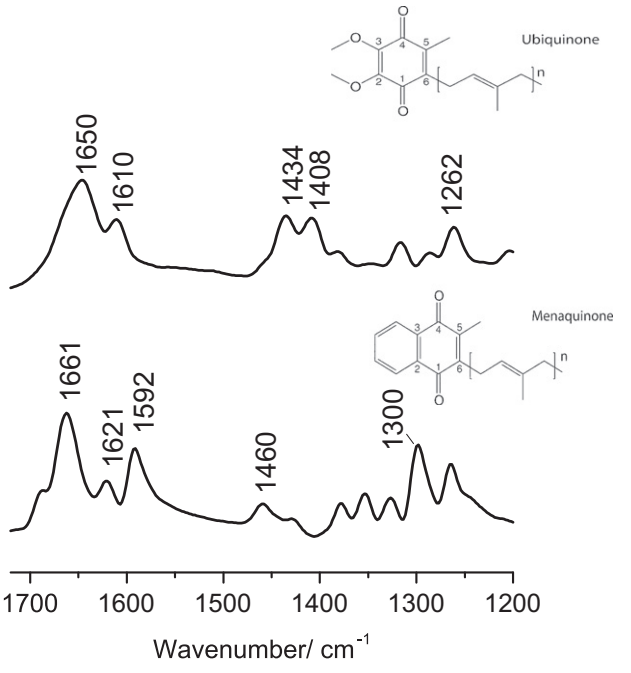

Fig. 1. Absorption spectra of UQ_{10} and MQ obtained in ethanol on an ATR reflection unit. The ethanol contributions are subtracted.

Table 1
Overview on values found for the ν(C═O) of vibrational mode of UQ and MQ in different proteins from the respiratory chain.

Sample	ν(C═O) of UQ/cm^{-1}	MQ	ref
In solution	1650	1670	[83] (and ref within)
QA *R. sphaeroides*	1660 (C1═O)	1651	[83]
	1601 (C4═O)	1640	
QB *R. sphaeroides*	1641 (C1═O)		[83]
	1641 (C4═O)		
QB *R. viridis*	1641 (C1═O)	1653	[83]
	1641 (C4═O)	1636	
bo_3 oxidase *E. coli*	1658 (C1═O)		[25]
	1658 (C4═O)		
bd oxidase *E. coli*	1666	1656	[63]
bc_1 *P. denitrificans*	1658/1644		[27]
bc_1 *R. capsulatus*	1666/1650		[77–79]
bc_1 bovine	1656		[80]
QFR *E. coli*	1666/1644	1646	[54]

signal at 1650 cm^{-1} in free quinone, may shift by about 25 cm^{-1} depending on the environment in the protein.

Isotope labeling was often used to identify the C═O group of ubiquinones and the binding geometry in the difference spectra of proteins [12,22–25]. As calculations on isolated Q show, the C═O and C═C modes mix with methoxy methyl CH bending vibrations, and in addition the degree of mixing is altered upon isotope labeling, resulting in complicated changes in mode frequencies, intensities, and composition upon isotope labeling [12,14]. Furthermore it was described that intensity changes of the C═O vibrational mode in a probed protein may point towards a specific orientation of the methoxy site chains [15,26]. The second characteristic spectral feature is the C═C vibration expected around 1610 cm^{-1}. It is as such not directly sensitive to hydrogen bonding. Due to the coupling to the CO vibrational modes, mentioned above, it was found shifted when the C═O groups were specifically isotopically labeled.

In the 1500–1300 cm^{-1} range, seen in Fig. 1, modes from the ring bonds (C–C), as well as from CH_2 and CH_3 groups, contribute [14,23,29]. In IR absorption spectra of isolated ubiquinones, bands at 1449–1436 cm^{-1} and at 1381 cm^{-1} have been previously attributed to δCH_2 and δCH_3 modes from the hydrocarbon chain and the 5-methyl substituent. The C–O–CH_3 vibrational mode can be identified around 1264 cm^{-1} in an often less crowded area of protein difference spectra. Interestingly the position and the intensity of this vibrational mode seem to be essentially unaffected upon binding and can be used to study the amount of quinone bound to the protein [27]. An example is shown in Fig. 2 below for the bc_1 complex from *Paracoccus denitrificans*. In the preparation studied here, the presence of 2 Q per bc_1 monomer was calculated.

In the spectra of menaquinone (Fig. 1B), the split ν(C═O) mode is observed at 1670 cm^{-1} with a shoulder at 1658 cm^{-1}. The ν(C═C) mode of the quinoid ring is found at 1624 cm^{-1}, and that of the aromatic ring is at 1596 cm^{-1}. The mode at 1304 cm^{-1} can be corroborated with a coupled C–C/C═C vibration [22].

2.2. Infrared data on quinols

Electrochemical studies of the double reduction of ubiquinone-2 (Q_2) in aqueous solution have been reported and QH_2 bands have been described at 1490, 1470, 1432 and 1388 cm^{-1}. [28,29]. Fig. 3 shows the electrochemically induced FTIR difference spectra of quinone in aqueous solution. The 1490 cm^{-1} band can be attributed to a ring C–C mode coupled to a C–OH mode. On the other hand, the 1470, 1433 and 1375 cm^{-1} ubiquinol bands observed in model compound studies, and which were found not to be sensitive to $^1H/^2H$ exchange, have been assigned to the reorganization of ring C–C (at 1470 and 1433 cm^{-1}), and CH_2/CH_3 (at 1433 and 1375 cm^{-1}) modes upon Q reduction [30].

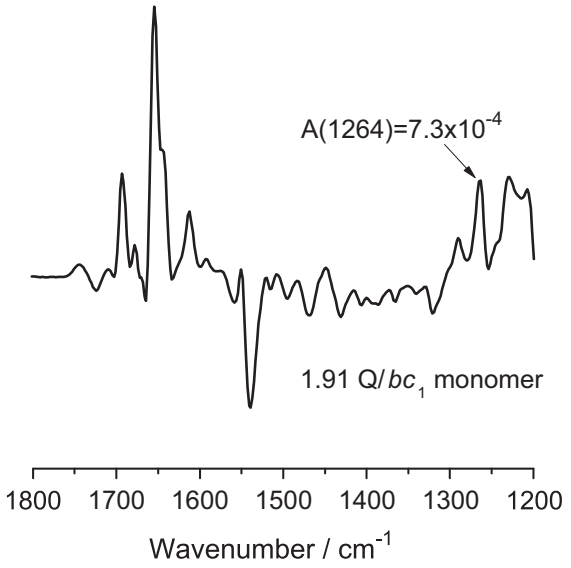

Fig. 2. Oxidized-minus reduced FTIR difference spectra of the bc_1 complex from *P. dentrificans*. The 1264 cm^{-1} signal used for the analysis of the ubiquinone content is highlighted.

Electrochemically induced FTIR difference spectra of site-specific ^{13}C-labeled UQ_2 at the C1═O or C4═O showed QH_2 bands at 1484, 1464, 1426 and 1384–1380 cm^{-1} [22–25]. The main QH_2 bands are therefore downshifted by ~6 cm^{-1} upon specific ^{13}C-labeling of either the C1- or the C4-carbonyl of Q_2, which is consistent with their assignments to ring C–C and $\delta CH_2/\delta CH_3$ modes [25]. Some of these modes have been suggested to be coupled to the OH/C–OH vibrations of the QH_2.

In the FTIR redox difference spectrum of menaquinone, the ν(C═O) mode is observed at 1670 cm^{-1} which is found at the same position as in the absorption spectra discussed above (Fig. 3). Similarly to ubiquinone the C═O group position and intensity depends on the hydrogen bonding environment and the geometry of the binding site, however, this was significantly less studied. The negative signals between 1450 and 1300 cm^{-1} can be corroborated with the signals of the quinoid ring.

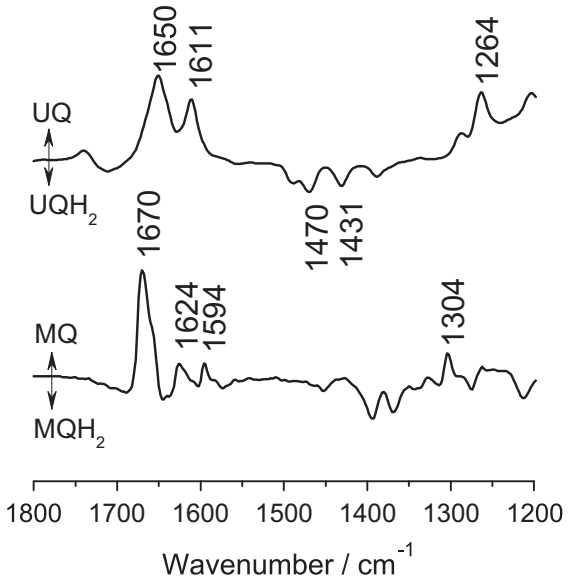

Fig. 3. Oxidized minus reduced FTIR difference spectra of UQ and MQ in phosphate buffer at pH 7 for the full potential step. The positive signals correlate with the neutral quinone and the negative signals with the fully protonated and reduced quinol.

The conversion of quinone to quinol includes the transfer of two electrons and protons. In proteins the intermediate state, as for example the semiquinone form can be found to be stabilized. These intermediates have also been extensively investigated by means of infrared spectroscopic approaches for the analysis of systems from photosynthesis (see for example [7,13,23,29,30]. Experimental data and calculations are also available on naphtoquinones and other quinone derivatives. However, since this review focusses on respiration we will essentially discuss the spectral signatures of reduced and oxidized ubiquinone and menaquinone.

3. Vibrational signature of quinones in different proteins from the respiratory chain

3.1. Identification of binding sites

In order to understand how quinones interact with proteins, it is important to identify the interaction partners and the factors that rule quinone orientation in the site. Often the combination of different techniques was necessary to study the position and the function of a quinone binding site. For example in the bo_3 oxidase from *Escherichia coli* the quinone binding sites have been analyzed by crystallographic, spectroscopic and biochemical studies leading to the suggestion that the quinone-binding sites are located close to the low-spin heme B in subunit I and a second one close to subunit II.

The purified bo_3 oxidase contains a tightly bound UQ_8 [31], which can be stabilized as an ubisemiquinone radical during enzymatic turnover [32,33]. Sato-Watanabe et al. [31] reported about a high affinity quinone binding site (QH) in vicinity to the low spin heme b by means of Raman spectroscopies. On the basis of the crystal structure, biochemical and EPR spectroscopic studies the residues participating to this high-affinity quinone binding site [34–36] have been identified. Sato-Watanabe et al. [31] postulated that the QH site serves as a transient electron reservoir for the two-electron supply from the low affinity site (QL) and gates electron transfer, allowing sequential one-electron transfer from the QL site to heme b. In an alternative explanation the second bound quinone seems to be able to rapidly exchange with the substrate pool [37]. The QL site was proposed to be located close to the QH site [37] by EPR spectroscopies or in the C-terminal hydrophilic domain of subunit II by photoaffinity cross-linking [38,39] and mutagenesis studies [40,41].

Selective ^{13}C-labeling of the bound ubiquinone in cytochrome bo_3 allowed depicting the vibrational modes of the ubiquinone from the overall contribution of the protein in electrochemically induced FTIR difference spectra [25]. On the basis of the experiments with the specifically ^{13}C-labeled UQ_2 analogues, the two carbonyl modes could be distinguished and the mainly symmetrical binding of the ring portion to the binding pocket was revealed.

Mutants in the vicinity of the QH binding sites have then been studied. In electrochemically induced FTIR difference spectra on the highly conservative D75E mutant enzyme, the shifts of signals from 1734 to 1750 cm^{-1} have been identified in direct comparison to wild type [42]. These modes, concomitant with the reduced state of the enzyme, could be assigned to the ν(C═O) vibrational mode of protonated D75 and E75, respectively. In the spectroscopic region where signals for deprotonated acidic groups were expected, bands shifted for the $\nu(COO^-)_{s/as}$ modes from 1563 to 1554–1539 cm^{-1} and from 1315 to 1336 cm^{-1}, for the oxidized enzyme, indicating that D75 is deprotonated in the oxidized form of cytochrome bo_3 and is protonated upon full reduction of the enzyme. The infrared spectroscopic data provides strong support for the proton uptake of D75 upon reduction of the bound ubiquinone at the high affinity site. EPR spectroscopies confirmed the important role of D75 for the catalytic reaction of the quinone radical that is suggested to be binding in an anionic rather than a neutral protonated form [36].

3.2. Accommodation of different quinone types in E. coli complexes

Another question that was addressed by means of infrared difference spectroscopy is the possibility of facultative anaerobic bacteria and lower eukaryotes to adapt their metabolism in response to environmental changes. An important aspect of this adaptability is that many bacteria can synthesize both ubiquinone (UQ) and menaquinone (MQ) [43]. This is also the case for *E. coli*, where, depending on the growing conditions, different quinone types are found in the membrane. Three types of quinones are synthesized: the benzoquinone ubiquinone (UQ_8) and two naphthoquinones, demethylmenaquinone (DMQ) and menaquinone (MQ). The composition varies depending upon the aerobic–anaerobic environment of the cell. Ubiquinone (UQ) and DMQ dominate under aerobic conditions, comprising ~65 and 32% of the quinone pool, with the remaining ~3% being MQ. This ratio changes, however, upon the switch to a more anoxic environment with about a 20-fold increase in MQ levels, a slight 1.5–2-fold increase in DMQ, and an 8-fold reduction in UQ [44–47].

Importantly some membrane-bound bacterial enzymes can catalyze redox reactions with both UQ and MQ despite the different structures and midpoint potentials. Quinones vary in redox potential (pH 7) with MQ (Em = ~−80 mV) having the lowest potential and DMQ (Em = ~+40 mV) and UQ (Em = ~+110 mV) having higher potential [45,46]. Although the redox properties of quinones depend for a large part on their chemical nature, it is also clear that the interactions between the quinone and the protein at a specific binding site can further modulate the electronic properties and thus the redox potential of this cofactor in situ. In general the modulation of the quinone midpoint potential may for example be induced by the orientation of the side chains in the protein site. It was reported that the difference in the redox potentials of up to 70 mV between the two quinones bound to the bacterial reaction center is related to differences in methoxy group conformations [48]. In order to bind both types of quinone, ubiquinol and menaquinol, the presence of two different sites may be suggested. Alternatively a structural change within one site may occur allowing the rearrangement due to the structural and steric differences between the one- and two-ring quinone systems.

Membrane-bound quinol–fumarate reductase (QFR) in *E. coli* is an example of an enzyme that can readily use both types of quinones and shows high menaquinol–fumarate and succinate–quinone reductase activities [49]. The X-ray structure of the four subunit complexes in *E. coli*, was solved revealing that the FrdA and FrdB subunits comprise the soluble component that contains a dicarboxylate substrate binding site, a covalently bound FAD, and three linearly arranged iron–sulfur centers [50]. The membrane-spanning hydrophobic subunits FrdC and FrdD, necessary to anchor the soluble FrdAB domain to the membrane, were found to harbor two menaquinone binding sites. However, only the proximal quinone binding site (Q_P), that is positioned proximal to the [3Fe–4S] cluster of the FrdB subunit, comprises a catalytically active site [51].

Electrochemically induced FTIR difference spectra of the QFR in the presence of ubiquinone or menaquinone revealed changes related to the interaction with the protein (Fig. 4). The most prominent signal that could be depicted was a vibrational mode of 1518 cm^{-1} characteristic for a protonated tyrosine residue and of 1498 cm^{-1} characteristic for the deprotonated form, that is shifted in wild-type and the Tyr-C25 and Asp-D88 mutants in the presence of MQ [52–54]. Interestingly, the Tyr-C25 side chain in QFR is located within 5 Å of the important residue Glu-C29 carboxyl on the polar side from the Q_P pocket. It is also hydrogen-bonded to Asp-D88 that is close to the protein surface where its protons could exchange with bulk solvent. On this basis it may be suggested that Tyr-C25 is a part of the proton-transfer pathway [54].

Kinetic measurements and docking studies of site specific mutations at the quinone binding site revealed that the ubiquinone and the menaquinone reduction does not take the same pathway for the proton

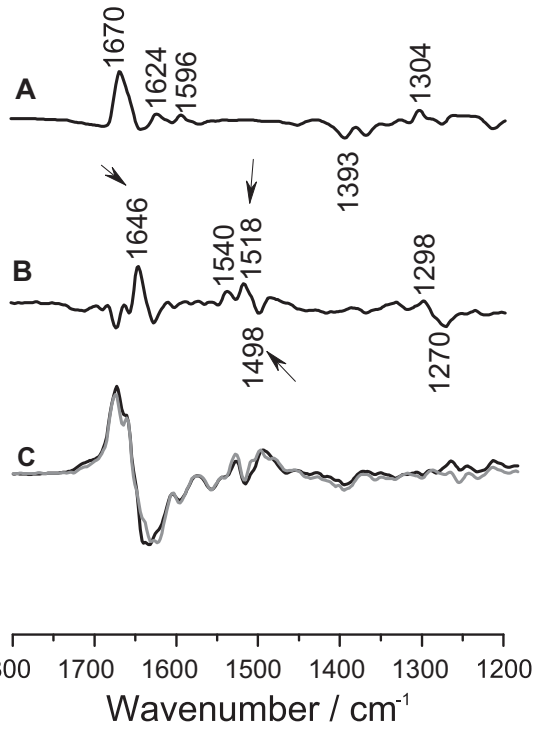

Fig. 4. Oxidized minus reduced FTIR difference spectra of menaquinone (A) and the double difference spectrum obtained when subtracting the difference spectra obtained QFR from *E. coli* in the presence and absence of menaquinone (B) as well as the data that was used for the subtraction (C).

transfer confirming that the site accommodates to the type of quinone used [55]. Importantly, not an individual residue functions as a partner for proton uptake; but several residues seem to be able to take this role. The flexibility of the quinone binding site was then suggested to be an evolutionarily conserved mechanism not only for maximizing, but also for regulating respiratory function [55].

A second example of a protein, where the accommodation of both UQ and MQ was studied by means of infrared spectroscopy, is cytochrome *bd*, a widely distributed bacterial oxidase [56]. In the respiratory chain of *E. coli*, the *bd* oxidase is expressed under microaerophilic growth conditions [57–60]. No crystal structure is available for the *bd* oxidase yet, but a hydrophilic loop, between transmembrane helices VI and VII in subunit I (the "Q loop"), was shown to be necessary for quinol oxidation, and probably comprises part of a quinol binding site [61]. The *bd* oxidase seems to be able to accommodate a semiquinone radical [62].

In the electrochemically induced FTIR difference spectra of *bd* oxidase, seen in Fig. 5 for the aerobically and the anaerobically grown *E. coli*, the changes of the quinone type can be clearly depicted and modes typical for ubiquinone (Fig. 5A) and menaquinone (Fig. 5B) arise. Interestingly, it was found that a mode at positive 1734 cm^{-1} is increased for the anaerobic form in Fig. 5B. The subtraction of the two difference spectra highlights this change and a negative mode appears in Fig. 5C. The signal is found at a position characteristic for protonated acidic residues. At the same time the negative signal seen at 1595 cm^{-1} in Fig. 5A, is absent in the spectra in the presence of menaquinone and correspondingly a negative signal is seen in the respective double difference spectra in Fig. 5C. These signals indicate a change in the protonation state of an aspartic or glutamic acid depending on the presence of ubiquinone or menaquinone [63].

When comparing the two studies on the *bd* oxidase and QFR it can be concluded that in both cases the site is able to adapt to the different quinone types. Whereas in the *bd* oxidase the protonation change of an acidic residue is observed, in the QFR a tyrosine residue seems to reorganize. This is not surprising since the binding site of quinones does

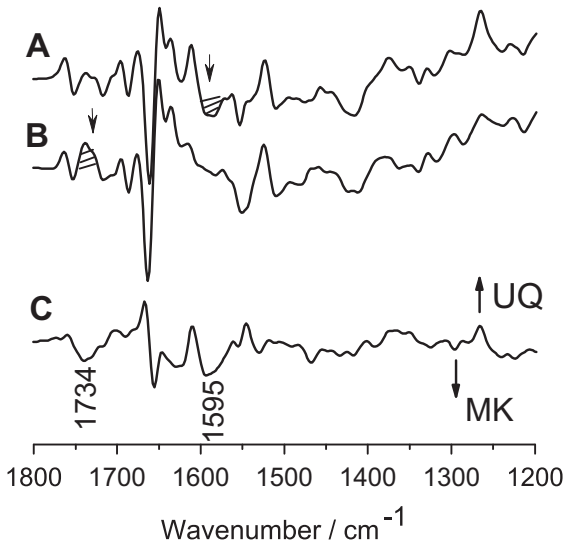

Fig. 5. Oxidized minus reduced FTIR difference spectra of aerobically (A) and anaerobically grown (B) *bd* oxidase from *E. coli*. The double difference spectra (C) highlight the vibrational modes of the two quinones and the differences in the protein environment upon change of quinone type.

not seem to have one common binding motif. The presence of some different motif types has been suggested [64]. In order to identify interaction principles, studies on other enzymes able to accommodate different quinones would be interesting, as for example the NADH ubiquinone reductase, complex I, where ubiquinone signals have been identified [65].

3.3. Interaction with inhibitors — the bc_1 complex

Ubiquinol–cytochrome *c* oxidoreductase (cytochrome bc_1 complex; complex III) is a fundamental component of the respiratory electron transfer chains located in the inner mitochondrial or bacterial cytoplasmic membrane. The crystal structures of several complexes have been reported (for example [66] and for review see [67]). All the bc_1 complexes contain at least the three catalytic subunits: cytochrome c_1 with covalently bound *c*-type heme, cytochrome *b* with two *b*-type hemes (b_L and b_H), and the Rieske iron sulfur protein with a [2Fe–2S] cluster. The enzyme couples the electron transfer from ubiquinol to cytochrome *c* to the translocation of protons across the membrane. Both bacterial and mitochondrial bc_1 complexes follow the same catalytic mechanism, the so-called Q-cycle which relies on two separate binding sites for quinones, Qo and Qi [68–70]. The Qo site is located close to heme b_L and the [2Fe–2S] cluster, and the Qi site is close to heme b_H on the opposite side of the membrane. Although this mechanism is generally accepted, various models for the quinol oxidation mechanism at the Qo site have been discussed (see for example [71–75]). Inhibitors provide an important tool to analyze the molecular mechanism of the bc_1 complex and have been extensively used to characterize the different quinone binding sites.

The crystal structure of the bc_1 complex from Yeast with natural stigmatellin A bound at the Qo site showed tight and specific binding of the inhibitor with the position of the conjugated trienes stabilized by several van der Waals interactions with cytochrome *b* residues [66]. The chromone head group was found to be stabilized by numerous nonpolar and a few polar interactions, including a hydrogen bond from the carbonyl group (4-CO) to His181, one of the [2Fe–2S] cluster ligands of the Rieske protein, which is thereby fixed in docking position on cytochrome *b* [66]. FTIR difference spectra obtained on bacterial [27,76–79] and mitochondrial bc_1 complexes [80] clearly revealed the presence of signals of the quinone(s) in the bc_1 complex. The number of quinones found depended on the organism and on the purification protocol. For the bc_1 complex from *P. denitrificans* 2–3 quinones have been identified [27]. For the bc_1 complex from *Rhodobacter capsulatus* a number of around 6–8 per monomer were reported, revealing not specifically bound quinone molecules [78]. The presence of nonspecifically bound quinone molecules has to be carefully taken into account when infrared data is interpreted, also in the case of other proteins. For the bc_1 complex we will thus review here mainly the data on the inhibitor interaction and on some of the mutants close to the quinone binding site.

FTIR difference spectroscopy was combined with isotope labeling of a modified Qo site inhibitor, undecylstigmatellin, to monitor the conformational changes of the protein upon inhibitor binding and identify redox-dependent alterations in the protonation state of acidic residues [76]. The comparison of spectra obtained from wild type and the bc_1 complex inhibited with natural stigmatellin A, ^{12}C- and ^{13}C-undecylstigmattelin, lead to the assignment of protein-specific features changes upon inhibitor binding. The inhibitors were found to be redox active, and the assignment of shifts from bands derived from stigmatellin itself was possible. It is noted, that these observations show that the co-reduction of stigmatellin has to be regarded in studies where the reduction of the enzyme in the presence of inhibitor is monitored.

In the electrochemically induced FTIR difference spectra described in Ritter et al. [76], several signals could be attributed to variations occurring in the presence of the inhibitors. The protein specific changes include the decrease of a signal at 1746 cm^{-1} when stigmatellin is bound, whereas a signal at 1736 cm^{-1} arises, as can be seen in Fig. 6 and the inset. These signals are located in a spectral region that exclusively includes contributions from protonated acidic groups, providing evidence that the binding of the inhibitor affects one or two protonated side chains. To interpret these spectral changes, two different scenarios can be considered. One explanation could be that the binding of inhibitor induces an environmental change of a protonated residue, leading to weaker hydrogen bonding and inducing the downshift of the ν(C═O) vibrational mode. Alternatively, the decrease of a signal at 1746 cm^{-1} was explained as deprotonation of an acidic residue, whereas the emerging signal at 1736 cm^{-1} would be derived from protonation of another residue. E272 (numbering for yeast) was shown to be a direct interaction partner to the hydroxyl group of stigmatellin [76] and thus was suggested to be deprotonated. It is possibly at the origin of the shifts seen here.

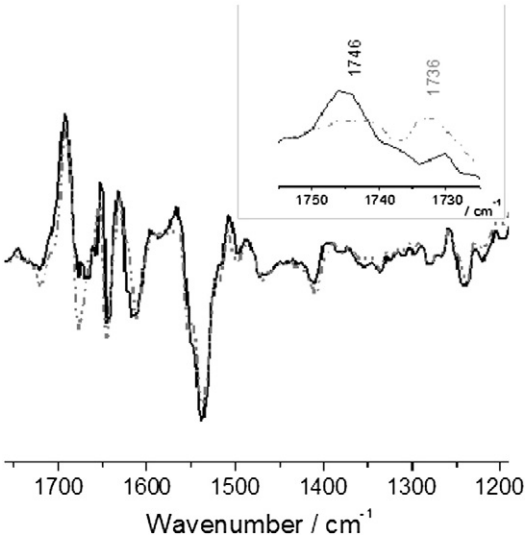

Fig. 6. Oxidized minus reduced FTIR difference spectra of wild type bc_1 complex from *S. cerevisiae* in the absence (full line) and presence of stigmatellin (dotted line). The inset shows the enlarged view of the spectral region characteristic for the protonated acidic residues.

The contribution of residues from the Qo binding site to this spectral range and their protonation state was further probed in the bc_1 complex from *P. denitrificans* [81]. On the basis of the comparison of the electrochemically induced FTIR difference spectra of the wild type (Fig. 7A) with the E295Q (B) and the D278N (C) mutant enzymes, it was discussed that these residues may be protonated in the oxidized form and thus be contributing to the signal at 1746 cm^{-1} in wild type as the signal was found to be decreased for both mutants. Alternatively it was suggested that the mutations perturb the local environment of protonated residues. Interestingly in both mutants the vibrational marker of the two C═O groups of the quinone, seen as a sharp signal at 1658 cm^{-1} in the wild type is significantly broader in the mutants (Fig. 7), indicating that one of the C═O groups experiences a weaker hydrogen bonding.

Finally the interaction of the wild-type enzyme from *P. denitrificans* with the inhibitor stigmatellin was monitored. The infrared difference spectra of the above Qo site mutations in the presence of stigmatellin confirm the previously established role of E295 (E272 in yeast) as a direct interaction partner in the enzyme from *P. denitrificans*. The protonated residue E295 was proposed to change the hydrogen-bonding environment upon stigmatellin binding in the oxidized form, and to be deprotonated in the reduced form. This was also confirmed for the *R. capsulatus* enzyme [79] when a full potential step is applied to reduce the enzyme, but could not be confirmed when studying partial redox reactions of the enzyme only [82].

The identification of the interaction of enzymes from the respiratory chain with inhibitors was also possible with the *bd* oxidase, where the presence of HQNO and the specific inhibitor Aurachin D was probed [63]. Similarly changes of the bound quinone modes were found. However it could be reported that the quinone is not completely removed due to the addition of the inhibitor.

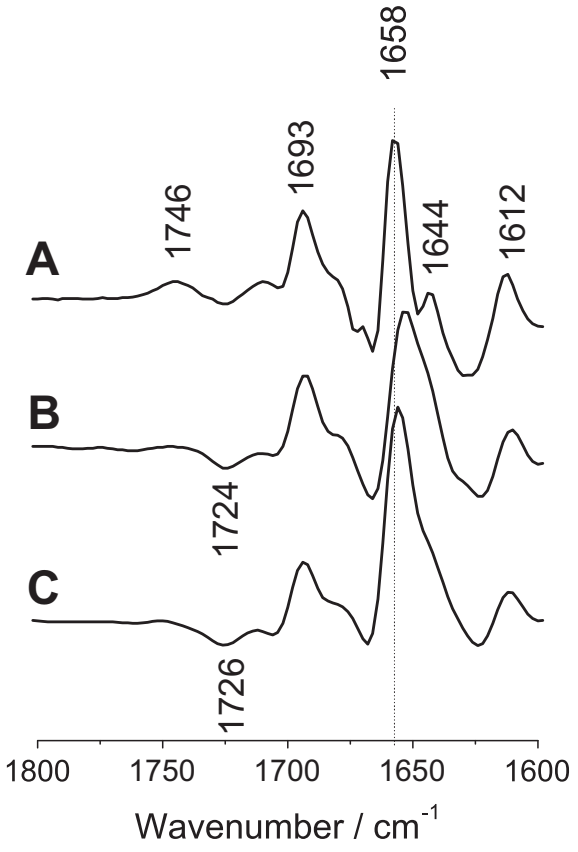

Fig. 7. Oxidized minus reduced FTIR difference spectra of the wild type bc_1 from *P. denitrificans* (A) in comparison to the E295Q (B) and D278N (C) mutant enzymes. The line indicates the C═O vibration of UQ, shifted upon mutation.

4. Conclusions

This review focusses on the infrared spectroscopic studies of quinones in proteins from the respiratory chain. Electrochemically or light induced FTIR difference spectroscopy is established as a technique that provides information on the type of quinone present in the sample. It is a method able to contribute to the understanding of the geometry of the binding site as the two C═O groups may be distinguished when introducing isotopically labeled quinones and when perturbing the site with site directed mutants. It was described that reaction induced infrared difference spectra reflect conformational and protonation changes that may occur upon an induced perturbation, such as a mutation, the binding of an inhibitor or the change of the type of quinone. On this basis the interesting question of the accommodation of different types of quinones and the plasticity of the quinone binding site was studied.

Acknowledgements

PH acknowledges the Institute Universitaire de France (IUF), the FRC Strasbourg, the University of Strasbourg and the CNRS for the financial support.

References

[1] B.L. Trumpower, Function of Quinones in Energy Conserving Systems, Academic Press, New York, 1982.
[2] F. Siebert, W. Mäntele, K. Gerwert, Fourier-transform infrared spectroscopy applied to rhodopsin. The problem of the protonation state of the retinylidene Schiff base reinvestigated, Eur. J. Biochem. 136 (1983) 119–127.
[3] K.J. Rothschild, W.A. Cantore, H. Marrero, Fourier transform infrared difference spectra of intermediates in rhodopsin bleaching, Science 219 (1983) 1333–1335.
[4] F. Siebert, W. Mäntele, Investigation of the primary photochemistry of bacteriorhodopsin by low-temperature Fourier-transform infrared spectroscopy, Eur. J. Biochem. 130 (1983) 565–573.
[5] M.S. Braiman, T. Mogi, T. Marti, L.J. Stern, H.G. Khorana, K.J. Rothschild, Vibrational spectroscopy of bacteriorhodopsin mutants: light-driven proton transport involves protonation changes of aspartic acid residues 85, 96, and 212, Biochemistry 27 (1988) 8516–8520.
[6] E. Nabedryk, C. Berthomieu, A. Verméglio, J. Breton, Photooxidation of high-potential (c559, c556) and low-potential (c552) hemes in the cytochrome subunit of *Rhodopseudomonas viridis* reaction center. Characterization by FTIR spectroscopy, FEBS Lett. 293 (1991) 53–58.
[7] S. Buchanan, H. Michel, K. Gerwert, Light-induced charge separation in *Rhodopseudomonas viridis* reaction centers monitored by Fourier-transform infrared difference spectroscopy: the quinone vibrations, Biochemistry 31 (1992) 1314–1322.
[8] C. Berthomieu, R. Hienerwadel, Fourier transform infrared (FTIR) spectroscopy, Photosynth. Res. 101 (2009) 157–170.
[9] A. Barth, Infrared spectroscopy of proteins, Biochim. Biophys. Acta 1767 (9) (2007) 1073–1101.
[10] C. Kötting, K. Gerwert, Proteins in action monitored by time-resolved FTIR spectroscopy, ChemPhysChem 6 (2005) 881–888.
[11] W. Mäntele, Reaction-induced infrared difference spectroscopy for the study of protein function and reaction mechanisms, Trends Biochem. Sci. 18 (1993) 197–202.
[12] H. Lamichhane, R. Wang, G. Hastings, Comparison of calculated and experimental FTIR spectra of specifically labeled ubiquinones, Vib. Spectrosc. 55 (2) (2011) 279–286.
[13] H.P. Lamichhane, G. Hastings, Calculated vibrational properties of pigments in protein binding sites, Proc. Natl. Acad. Sci. 108 (26) (2011) 10526–10531.
[14] J.-R. Burie, A. Boussac, C. Boullais, G. Berger, T. Mattioli, C. Mioskowsky, E. Nabedryk, J. Breton, J. Phys. Chem. 99 (1995) 4059–4070.
[15] J.-R. Burie, C. Boullais, M. Nonella, C. Mioskowski, E. Nabedryk, J. Breton, Importance of the conformation of methoxy groups on the vibrational and electrochemical properties of ubiquinones, J. Phys. Chem. B 101 (1997) 6607–6617.
[16] G. Balakrishnan, P. Mohandas, S. Umpathy, Ab initio studies on structure and vibrational spectra of ubiquinone and its radical anion, Spectrochim. Acta A Mol. Biomol. Spectrosc. 53 (10) (1997) 1553–1561.
[17] T. Anno, A. Sado, Electronic states of p-benzoquinone. IV. Infrared spectrum and assignment of vibrational frequencies in the ground electronic state, Bull. Chem. Soc. Jpn. 31 (1958) 734.
[18] T. Anno, Molecular vibrations of quinones. V. Normal coordinate analysis of p-benzoquinone and its isotopic derivatives, J. Chem. Phys. 42 (1965) 932.
[19] E. Charney, E.D. Becker, Molecular vibrations of quinones. II. Infrared spectra (solution and vapor) of p-benzoquinone and p-benzoquinone-d4, J. Chem. Phys. 42 (1965) 910.
[20] H. Stammreich, R. Forneris, Das Raman-. Spektrum des p-Benzochinons, Z. Naturforsch. 7a (1959) 756.
[21] H. Stammreich, Th. Teixeira Sans, Molecular vibrations of quinones. IV. Raman spectra of p-benzoquinone and its centrosymmetrically substituted isotopic derivatives and assignment of observed frequencies, J. Chem. Phys. 42 (1965) 920.

[22] J. Breton, J.R. Burie, C. Berthomieu, G. Berger, E. Nabedryk, The binding sites of quinones in photosynthetic bacterial reaction centers investigated by light-induced FTIR difference spectroscopy: assignment of the QA vibrations in *Rhodobacter sphaeroides* using 18O- or 13C-labeled ubiquinone and vitamin K1, Biochemistry 33 (1994) 4953–4965.

[23] J. Breton, C. Boullais, J.R. Burie, E. Nabedryk, C. Mioskowski, Binding sites of quinones in photosynthetic bacterial reaction centers investigated by light-induced FTIR difference spectroscopy: assignment of the interactions of each carbonyl of QA in *Rhodobacter sphaeroides* using site-specific 13C-labeled ubiquinone, Biochemistry 33 (1994) 14378–14386.

[24] R. Brudler, H.J.M. de Groot, W.B.S. van Liemt, W.F. Steggerda, R. Esmeijer, P. Gast, A.J. Hoff, J. Lugtenburg, K. Gerwert, EMBO J. 13 (1994) 5523–5530.

[25] P. Hellwig, T. Mogi, F.L. Tomson, R.B. Gennis, J. Iwata, H. Miyoshi, W. Mäntele, Biochemistry 38 (1999) 14683–14689.

[26] C. Boullais, E. Nabedryk, J.-R. Burie, M. Nonella, C. Mioskowski, J. Breton, Site-specific isotope labeling demonstrates a large mesomeric resonance effect of the methoxy groups on the carbonyl frequency in ubiquinones, Photosynth. Res. 55 (2) (1998) 247–252.

[27] M. Ritter, O. Anderka, B. Ludwig, W. Mäntele, P. Hellwig, Electrochemical and FTIR spectroscopic characterization of the cytochrome bc_1 complex from *Paracoccus denitrificans*: evidence for protonation reactions coupled to quinone binding, Biochemistry 42 (42) (2003) 12391–12399.

[28] M. Bauscher, W. Maentele, Electrochemical and infrared-spectroscopic characterization of redox reactions of p-quinones, J. Phys. Chem. 96 (26) (1992) 11101–11108.

[29] M. Bauscher, E. Nabedryk, K. Bagley, J. Breton, W. Mäntele, Investigation of models for photosynthetic electron acceptors: infrared spectroelectrochemistry of ubiquinone and its anions, FEBS Lett. 261 (1) (1990) 191–195.

[30] A. Mezzetti, W. Leibl, J. Breton, E. Nabedryk, Photoreduction of the quinone pool in the bacterial photosynthetic membrane: identification of infrared marker bands for quinol formation, FEBS Lett. 537 (1–3) (2003) 161–165.

[31] M. Sato-Watanabe, T. Mogi, T. Ogura, T. Kitagawa, H. Miyoshi, H. Iwamura, Y. Anraku, Identification of a novel quinone-binding site in the cytochrome *bo* complex from *Escherichia coli*, J. Biol. Chem. 269 (1994) 28908–28912.

[32] M. Sato-Watanabe, S. Itoh, T. Mogi, K. Matsuura, H. Miyoshi, Y. Anraku, Stabilization of a semiquinone radical at the high-affinity quinone-binding site (Q_H) of the *Escherichia coli bo*-type ubiquinol oxidase, FEBS Lett. 374 (1995) 265–269.

[33] W.J. Ingledew, T. Ohnishi, J.C. Salerno, Studies on a stabilisation of ubisemiquinone by *Escherichia coli* quinol oxidase, cytochrome *bo*, Eur. J. Biochem. 227 (1995) 903–908.

[34] J. Abramson, S. Riistama, G. Larsson, A. Jasaitis, M. Svensson-Ek, L. Laakkonen, A. Puustinen, S. Iwata, M. Wikstrom, The structure of the ubiquinol oxidase from *Escherichia coli* and its ubiquinone binding site, Nat. Struct. Biol. 7 (2000) 910–917.

[35] P. Hellwig, T. Yano, T. Ohnishi, R.B. Gennis, Identification of the residues involved in stabilization of the semiquinone radical in the high-affinity ubiquinone binding site in cytochrome bo(3) from *Escherichia coli* by site-directed mutagenesis and EPR spectroscopy, Biochemistry 41 (2002) 10675–10679.

[36] F. MacMillan, S. Kacprzak, P. Hellwig, S. Grimaldi, H. Michel, M. Kaupp, Elucidating mechanisms in haem copper oxidases: the high-affinity Q_H binding site in quinol oxidase as studied by DONUT-HYSCORE spectroscopy and density functional theory, Faraday Discuss. 148 (2011) 315–344.

[37] L.L. Yap, M.T. Lin, H. Ouyang, R.I. Samoilova, S.A. Dikanov, R.B. Gennis, The quinone-binding sites of the cytochrome bo_3 ubiquinol oxidase from *Escherichia coli*, Biochim. Biophys. Acta 1797 (12) (2010) 1924–1932.

[38] R. Welter, C.Q. Gu, L. Yu, C.-A. Yu, J.N. Rumbley, R.B. Gennis, Identification of the ubiquinol-binding site in the cytochrome bo_3-ubiquinol oxidase of *Escherichia coli*, J. Biol. Chem. 269 (1994) 28834–28838.

[39] P.H. Tsatsos, K. Reynolds, E.F. Nickels, D.-Y. He, C.-A. Yu, R.B. Gennis, Using matrix-assisted laser desorption ionization mass spectrometry to map the quinol binding site of cytochrome bo_3 from *Escherichia coli*, Biochemistry 37 (1998) 9884–9888.

[40] M. Sato-Watanabe, T. Mogi, K. Sakamoto, H. Miyoshi, Y. Anraku, Isolation and characterizations of quinone analogue-resistant mutants of *bo*-type ubiquinol oxidase from *Escherichia coli*, Biochemistry 37 (1998) 12744–12752.

[41] J. Ma, A. Puustinen, M. Wikström, R.B. Gennis, Tryptophan-136 in subunit II of cytochrome bo_3 from *Escherichia coli* may participate in the binding of ubiquinol, Biochemistry 37 (1998) 11806–11811.

[42] P. Hellwig, B. Barquera, R.B. Gennis, Direct evidence for the protonation of aspartate-75, proposed to be at a quinol binding site, upon reduction of cytochrome bo_3 from *Escherichia coli*, Biochemistry 40 (4) (2001) 1077–1082.

[43] M.D. Collins, D. Jones, Distribution of isoprenoid quinone structural types in bacteria and their taxonomic implication, Microbiol. Rev. 45 (1981) 316–335.

[44] B.J. Wallace, I.G. Young, Aerobic respiration in mutants of *Escherichia coli* accumulating quinone analogues of ubiquinone, Biochim. Biophys. Acta 461 (1977) 75–83.

[45] R. Hollander, Correlation of the function of demethylmenaquinone in bacterial electron transport with its redox potential, FEBS Lett. 72 (1976) 98–100.

[46] G. Unden, J. Bongaerts, Alternative respiratory pathways of *Escherichia coli*: energetics and transcriptional regulation in response to electron acceptors, Biochim. Biophys. Acta 1320 (1997) 217–234.

[47] A.I. Shestopalov, A.V. Bogachev, R.A. Murtazina, M.B. Viryasov, V.P. Skulachev, Aeration-dependent changes in composition of the quinone pool in *Escherichia coli*. Evidence of post-transcriptional regulation of the quinone biosynthesis, FEBS Lett. 404 (2–3) (1997) 272–274.

[48] R.C. Prince, P.L. Dutton, J.M. Bruce, Electrochemistry of ubiquinones: menaquinones and plastoquinones in aprotic solvents, FEBS Lett. 160 (1983) 273–276.

[49] E. Maklashina, G. Cecchini, Comparison of catalytic activity and inhibitors of quinone reactions of succinate dehydrogenase (Succinate–ubiquinone oxidoreductase) and fumarate reductase (Menaquinol–fumarate oxidoreductase) from *Escherichia coli*, Arch. Biochem. Biophys. 369 (1999) 223–232.

[50] T.M. Iverson, C. Luna-Chavez, G. Cecchini, D.C. Rees, Structure of the *Escherichia coli* fumarate reductase respiratory complex, Science 284 (1999) 1961–1966.

[51] T.M. Iverson, C. Luna-Chavez, L.R. Croal, G. Cecchini, D.C. Rees, Crystallographic studies of the *Escherichia coli* quinol–fumarate reductase with inhibitors bound to the quinol-binding site, J. Biol. Chem. 277 (2002) 16124–16130.

[52] M. Wolpert, P. Hellwig, Infrared spectra and molar absorption coefficients of the 20 alpha amino acids in aqueous solutions in the spectral range from 1800 to 500 cm(−1), Spectrochim. Acta A 64 (2006) 987–1001.

[53] A. Barth, The infrared absorption of amino acid side chains, Prog. Biophys. Mol. Biol. 74 (2000) 141–173.

[54] E. Maklashina, P. Hellwig, R.A. Rothery, V. Kotlyar, Y. Sher, J.H. Weiner, G. Cecchini, Differences in protonation of ubiquinone and menaquinone in fumarate reductase from *Escherichia coli*, J. Biol. Chem. 281 (2006) 26655–26664.

[55] P.K. Singh, M. Sarwar, E. Maklashina, V. Kotlyar, S. Rajagukguk, T.M. Tomasiak, G. Cecchini, T.M. Iverson, Plasticity of the quinone-binding site of the complex II homolog quinol:fumarate reductase, J. Biol. Chem. 288 (2013) 24293–24301.

[56] S. Jünemann, Cytochrome *bd* terminal oxidase, Biochim. Biophys. Acta 1321 (1997) 107–127.

[57] Y. Anraku, R.B. Gennis, The aerobic respiratory chain of *Escherichia coli*, Trends Biochem. Sci. 12 (1987) 262–266.

[58] C.W. Rice, W.P. Hempfling, Oxygen-limited continuous culture and respiratory energy conservation in *Escherichia coli*, J. Bacteriol. 134 (1978) 115–124.

[59] T. Mogi, M. Tsubaki, H. Hori, H. Miyoshi, H. Nakamura, Y. Anraku, Two terminal quinol oxidase families in *Escherichia coli*: variations on molecular machinery for dioxygen reduction, J. Biochem. Mol. Biol. Biophys. 2 (1998) 79–110.

[60] J.J. Hill, J.O. Alben, R.B. Gennis, Spectroscopic evidence for a heme–heme binuclear center in the cytochrome *bd* ubiquinol oxidase from *Escherichia coli*, Proc. Natl. Acad. Sci. U. S. A. 90 (1993) 5863–5867.

[61] J.P. Osborne, R.B. Gennis, Sequence analysis of cytochrome *bd* oxidase suggests a revised topology for subunit I, Biochim. Biophys. Acta 1410 (1999) 32–50.

[62] S.F. Hastings, W.J. Ingledew, A study of the stabilization of semiquinones by the *Escherichia coli* quinol oxidase cytochrome *bd*, Biochem. Soc. Trans. 24 (1996) 131–132.

[63] J. Zhang, W. Oettmeier, R.B. Gennis, P. Hellwig, FTIR spectroscopic evidence for the involvement of an acidic residue in quinone binding in cytochrome *bd* from *Escherichia coli*, Biochemistry 41 (2002) 4612–4617.

[64] P. Rich, N. Fisher, Generic features of quinone-binding sites, Biochem. Soc. Trans. 27 (4) (1999) 561–565.

[65] D. Marshall, N. Fisher, L. Grigic, V. Zickermann, U. Brandt, R.J. Shannon, J. Hirst, R. Lawrence, P.R. Rich, ATR-FTIR redox difference spectroscopy of *Yarrowia lipolytica* and bovine complex I, Biochemistry 45 (17) (2006) 5458–5467.

[66] C. Hunte, J. Koepke, C. Lange, T. Rossmanith, H. Michel, Structure at 2.3 Å resolution of the cytochrome bc_1 complex from the yeast *Saccharomyces cerevisiae* cocrystallized with an antibody Fv fragment, Structure 8 (2000) 669–684.

[67] E.A. Berry, H. De Bari, L.S. Huang, Unanswered questions about the structure of cytochrome bc_1 complexes, Biochim. Biophys. Acta 1827 (2013) 1258–1277.

[68] P. Mitchell, Possible molecular mechanisms of the protonmotive function of cytochrome systems, J. Theor. Biol. 62 (1976) 327–367.

[69] B.L. Trumpower, The protonmotive Q cycle. Energy transduction by coupling of proton translocation to electron transfer by the cytochrome bc_1 complex, J. Bioenerg. Biomembr. 23 (1990) 241–255.

[70] U. Brandt, B. Trumpower, The protonmotive Q cycle in mitochondria and bacteria, Crit. Rev. Biochem. Mol. Biol. 29 (1994) 165–197.

[71] H. Ding, C.C. Moser, D.E. Robertson, M.K. Tokito, F. Daldal, P.L. Dutton, Ubiquinone pair in the Qo site central to the primary energy conversion reactions of cytochrome bc_1 complex, Biochemistry 34 (1995) 15979–15996.

[72] R.E. Sharp, B.R. Gibney, A. Palmitessa, J.L. White, J.A. Dixon, C.C. Moser, F. Daldal, P.L. Dutton, Effect of inhibitors on the ubiquinone binding capacity of the primary energy conversion site in the *Rhodobacter capsulatus* cytochrome bc_1 complex, Biochemistry 38 (1999) 14973–14980.

[73] X. Yang, B. Trumpower, Protonmotive Q cycle pathway of electron transfer and energy transduction in the three-subunit ubiquinol–cytochrome *c* oxidoreductase complex of *Paracoccus denitrificans*, J. Biol. Chem. 263 (1988) 11962–11970.

[74] A.R. Crofts, The Q-cycle — a personal perspective, Photosynth. Res. 80 (2004) 223–243.

[75] A. Osyczka, C.C. Moser, P.L. Dutton, Fixing the Q cycle, Trends Biochem. Sci. 30 (2005) 176–182.

[76] M. Ritter, H. Palsdottir, M. Abe, W. Mäntele, C. Hunte, H. Miyoshi, P. Hellwig, Direct evidence for the interaction of stigmatellin with a protonated acidic group in the bc_1 complex from *Saccharomyces cerevisiae* as monitored by FTIR difference spectroscopy and ^{13}C specific labeling, Biochemistry 43 (2004) 8439–8446.

[77] F. Baymann, D.E. Robertson, P.L. Dutton, W. Mäntele, Electrochemical and spectroscopic investigations of the cytochrome bc_1 complex from *Rhodobacter capsulatus*, Biochemistry 38 (1999) 13188–13199.

[78] M. Iwaki, A. Osyczka, C.C. Moser, P.L. Dutton, P.R. Rich, ATR-FTIR spectroscopy studies of iron–sulfur protein and cytochrome c_1 in the *Rhodobacter capsulatus* cytochrome bc_1 complex, Biochemistry 43 (2004) 9477–9486.

[79] D.W. Lee, Y. El Khoury, F. Francia, B. Zambelli, S. Ciurli, G. Venturoli, P. Hellwig, F. Daldal, Zinc inhibition of bacterial cytochrome *bc*1 reveals the role of cytochrome *b* E295 in proton release at the Q(o) site, Biochemistry 50 (2011) 4263–4272.

[80] M. Iwaki, L. Giotta, A.O. Akinsiku, H. Schägger, N. Fisher, J. Breton, P.R. Rich, Redox-induced transitions in bovine cytochrome bc_1 complex studied by perfusion-induced ATR-FTIR spectroscopy, Biochemistry 42 (2003) 11109–11119.
[81] T. Kleinschroth, O. Anderka, M. Ritter, A. Stocker, T.A. Link, B. Ludwig, P. Hellwig, Characterization of mutations in crucial residues around the Q_o binding site of the cytochrome bc_1 complex from *Paracoccus denitrificans*, FEBS J. 275 (2008) 4773–4785.
[82] A. Osyczka, H. Zhang, C. Mathé, P.R. Rich, C.C. Moser, P.L. Dutton, Role of the PEWY glutamate in hydroquinone–quinone oxidation–reduction catalysis in the Q_o Site of cytochrome bc_1, Biochemistry 45 (2006) 10492–10503.
[83] J. Breton, E. Nabedryk, Protein–quinone interactions in the bacterial photosynthetic reaction center: light-induced FTIR difference spectroscopy of the quinone vibrations, Biochim. Biophys. Acta Bioenerg. 1275 (1996) 84–90.